Published in final edited form as:
J Immunol. 2010 February 15; 184(4): 2014–2025. doi:10.4049/jimmunol.0900183.

Influenza Virus-Specific Immunological Memory Is Enhanced by Repeated Social Defeat

Jacqueline W. Mays[*], **Michael T. Bailey**[*,†,‡], **John T. Hunzeker**[§], **Nicole D. Powell**[*], **Tracey Papenfuss**[‡,¶], **Erik A Karlsson**[‖], **David A. Padgett**[*,†,‡], and **John F. Sheridan**[*,†,‡]

[*]Section of Oral Biology, College of Dentistry, The Ohio State University, Columbus, OH 43210

[†]Department of Molecular Virology, Immunology and Medical Genetics, The Ohio State University, Columbus, OH 43210

[‡]Institute for Behavioral Medicine Research, College of Medicine, The Ohio State University, Columbus, OH 43210

[¶]Department of Veterinary Biosciences, College of Veterinary Medicine, The Ohio State University, Columbus, OH 43210

[§]The Pennsylvania State University College of Medicine, Hershey, PA 17033

[‖]Department of Nutrition, Gillings School of Global Public Health, University of North Carolina, Chapel Hill, NC 27599

Abstract

Immunological memory (MEM) development is affected by stress-induced neuroendocrine mediators. Current knowledge about how a behavioral interaction, such as social defeat, alters the development of adaptive immunity, and MEM is incomplete. In this study, the experience of social disruption stress (SDR) prior to a primary influenza viral infection enhanced the frequency and function of the T cell memory pool. Socially stressed mice had a significantly enlarged population of $CD8^+$ T cells specific for the immunodominant NP366–74 epitope of A/PR/8/34 virus in lung and spleen tissues at 6–12 wk after primary infection (resting memory). Moreover, during resting memory, SDR-MEM mice responded with an enhanced footpad delayed-type hypersensitivity response, and more IFN-γ–producing $CD4^+$ T cells were detected after ex vivo stimulation. When mice were rechallenged with A/PR/8/34 virus, SDR-MEM mice terminated viral gene expression significantly earlier than MEM mice and generated a greater $D^bNP_{366–74}CD8^+$ T cell response in the lung parenchyma and airways. This enhancement was specific to the T cell response. SDR-MEM mice had significantly attenuated anti-influenza IgG titers during resting memory. Similar experiments in which mice were primed with X-31 influenza and challenged with A/PR/8/34 virus elicited similar enhancements in the splenic and lung airway D^b $NP_{366–74}CD8^+$ T cell populations in SDR-MEM mice. This study demonstrates that the experience of repeated social defeat prior to a primary viral infection significantly enhances virus-specific memory via augmentation of memory T cell populations and suggests that social stressors should be carefully considered in the design and analysis of future studies on antiviral immunity.

Address correspondence and reprint requests to Dr. John F. Sheridan, Section of Oral Biology, College of Dentistry, The Ohio State University, P.O. Box 182357, Columbus, OH 43218. sheridan.1@osu.edu.

The online version of the article contains supplemental material.

Disclosures

The authors have no financial conflicts of interest.

Influenza viral infection continues to be a serious worldwide health threat that affects 20% of children and 5% of adults annually (1). Ongoing efforts are focused on better understanding the immune response to a primary influenza infection, as well as on elucidating factors that impact the quality and quantity of immunological memory established subsequent to a primary viral infection. Immune protection from an influenza infection is afforded by appropriate vaccination or prior infection with a similar virus. Critical components of the anti-influenza memory response include B cells and $CD4^+$ and $CD8^+$ T cells. These cells exist as memory cells after a primary influenza infection and are capable of rapid activation, clonal expansion, and mobilization upon re-encounter with a similar influenza virus. Upon reinfection, $CD4^+$ T cells direct the activation of memory B cells and $CD8^+$ T cells and support the antiviral activity of effector $CD8^+$ T cells via cytokine production (2). Activated $CD8^+$ T cells clonally expand, mature, and traffic to the site of infection, where they directly lyse virus-infected cells and release antiviral cytokines, including IFN-γ and TNF-α to perpetuate the cellular antiviral response (3). Memory $CD8^+$ T cells may be resident in lymphoid repositories or in peripheral tissues, including the lung parenchyma. Within the lung parenchyma, memory $CD8^+$ T cells can be quickly activated and expand to an effector population within the lung tissue (4–9). To manipulate these responses to improve antiviral therapy, it is crucial to gain a more complete grasp of the factors, including those beyond the immune system, which are able to regulate the immune response to a viral challenge.

Psychosocial stress is known to impact health, primarily via interactions among the nervous, endocrine, and immune systems that translate social experiences into physiological responses (10–12). Specific stress-reactive pathways, including the hypothalamic-pituitary-adrenal (HPA) axis and the sympathetic nervous system, facilitate intersystem communication via the release of glucocorticoids (GCs), catecholamines, and cytokines (13,14). These neuroendocrine mediators enable environmental interactions to directly affect the course of a primary viral infection and the subsequent development of memory (15,16). The respiratory tract is an area rich in sympathetic innervation, and T and B cells, containing functional β_2 adrenergic receptors, have been found in close contact with sympathetic nerve termini (13,17–20). Abundant lung vascularization allows ample exposure to serum factors, including corticosterone, an adrenal cortex hormone that results from HPA activation. The well-defined immunopathogenesis of the experimental influenza A/PR/8/34 mouse model provides a rich context in which to query the immunologic consequences of psychological stress, with a focus on lung tissue. Interestingly, viral infection alone is a well-established physiological stressor (21). To this end, circulating levels of the adrenal stress hormone corticosterone have been used as a surrogate measure of the severity of a viral infection via HPA activation (21).

Experimental stress paradigms have different effects on the immune system that depend, in large part, on the nature and duration of the stressor (22–24). Our laboratory has used a model of psychosocial stress that strongly impacts the immune system through activation of the HPA axis and the sympathetic nervous system. Social disruption stress (SDR) is a well-defined model of social stress that involves intermale aggression and results in the loss of social status, development of anxiety-like behavior, and enhanced inflammatory responses in male mice (25–27). Specific immunological changes that have been observed in mice following six cycles of SDR include: splenomegaly; elevated levels of circulating proinflammatory cytokines; enhanced expression of TLRs on bone marrow, blood, and splenic monocytes; and the development of functional GC resistance (27–31). In SDR mice, the circadian rhythm of the HPA axis is maintained, and normal immune regulation by corticosterone is typically restored by 30 d after the conclusion of the last stress cycle (32). Work in the SDR model has focused on SDR-induced alterations within the innate immune system (31). The impact of these changes on the adaptive antiviral responses and the

subsequent development of MEM is unknown. However, SDR-enhanced proinflammatory cytokine responses, in conjunction with an attenuated response to the intrinsic anti-inflammatory GC circuit, set the stage for a hyperactivated immune response with potential to enhance the adaptive immune response to a viral infection (33–37). The pattern and size of the virus-specific $CD8^+$ T cell memory pool are determined by the adaptive response to the primary viral challenge. Therefore, SDR-induced changes to a primary influenza infection are expected to modulate memory (38). In preliminary studies of a primary A/PR/8 viral infection, we observed reduced morbidity in SDR mice that was followed by an enhanced resistance to viral rechallenge. Therefore, we hypothesized that the immune changes observed subsequent to SDR would positively affect the establishment of the anti-influenza memory.

The present study was designed to investigate the effect of repeated social disruption, prior to a sublethal primary influenza viral infection, on the development and function of virus-specific memory. The studies described herein focused on the $CD8^+$ T cell component of the memory response, because tools were available to quantify the magnitude of this response. $D^bNP_{366–74}$ $CD8^+$ T cells are specific for the immunodominant epitope of the A/PR/8 virus, nucleoprotein 366–74, in C57/BL/6 mice (39). During resting memory and throughout a viral rechallenge, more virus-specific $D^bNP_{366–74}$ $CD8^+$ T cells were detected in the lung, with more of these cells expressing a memory (MEM) phenotype: IL-$7R_{HI}$ (40,41). $CD4^+$ T cell memory was enhanced, as assessed by cell population analysis and footpad delayed-type hypersensitivity (DTH) challenge 6–8 wk after primary infection. Concomitant increases in the gene expression of antiviral (IFN-γ) and regulatory (IL-2) cytokines supported the lung-based memory $CD8^+$ T cell population observed in SDR-MEM. Functionally, exposure to SDR prior to primary infection resulted in earlier termination of viral gene expression following rechallenge. Thus, the robust antiviral $CD8^+$ T cell response to a viral rechallenge in SDR-MEM mice was enhanced in volume and function. This study demonstrates that social defeat, prior to a primary influenza viral infection, enhanced the epitope-specific $CD8^+$ T cell memory population in a manner localized within the lung parenchyma.

Materials and Methods

Mice

Male C57BL/6 (6–8 wk) mice were obtained from Charles River Laboratories (San Diego, CA). Three to five experimental animals were housed per cage in an American Association of Accreditation of Laboratory Animal Care-accredited facility; they had access to food and tap water adlibitum. Mice were allowed to acclimate to their surrounding for ≥1 wk prior to any manipulation and were maintained on a 12-h light/dark cycle with lights on at 6:00 AM.

Social disruption stress

The SDR paradigm has been described in detail (25,42). Briefly, mice underwent six consecutive cycles of SDR prior to infection. A single cycle of SDR consisted of placing an intruder into the cage of experimental mice from 5:00 to 7:00 PM. Intruders (aggressors) were individually housed C57BL/6 or CD-1 males, who were isolated subsequent to a history of antagonistic behavior. Sessions were monitored to ensure that the intruder repeatedly attacked and consistently defeated the resident mice. If the residents defeated the aggressor or if the aggressor did not attack the residents, the aggressor was removed and replaced by a different aggressor mouse. Behavioral analysis and neuroendocrine profiles for mice in these studies are expected to be similar to those previously published, which included increased anxiety-like behavior and a significant increase in circulating corticosterone and catecholamines (25,42,43). During SDR, the resident mice generally displayed submissive behaviors, including upright submissive posture, fleeing, and crouching (25,42). The

nonstress control group (MEM) was isolated from the stressor. All animal care procedures were according to guidelines established by the National Institutes of Health Guide for the Care and Use of laboratory animals; protocols were approved by the The Ohio State University Institutional Laboratory Animal Care and Use Committee.

Virus and infection

For the primary infection, mice were infected 36 h after the conclusion of the last SDR cycle. Frozen stocks of influenza A/PR/8/34 virus were grown in the allantoic fluid of chicken eggs, as previously reported (44). Immediately prior to infection, mice were anesthetized by i.m. injection of ketamine/xylazine (78.1/4.4 mg/kg, Vedco, St. Joseph, MO) diluted in sterile saline. Intranasal infection with 1 hemagglutinating unit (HAU) of influenza A/PR/8/34 suspended in 50 μl sterile saline for the primary infection or 16 HAU the LD_{50} for this virus in a naive C57 mouse for rechallenge. For the heterologous prime-challenge experiments, H3N2 X-31 influenza virus, a generous gift from D. Woodland (Trudeau Institute, Saranac Lake, NY), was grown and titered as previously described (45). Three hundred 50% egg infectious dose was given intranasally for primary infection, followed by 3 HAU A/PR/8/34 for the memory challenge.

Anti-influenza IgG ELISA

Blood samples were collected from the retro-orbital capillary plexus immediately prior to sacrifice and were stored at 4°C overnight, after which serum was separated out and frozen until analysis by ELISA. Plates were coated with live influenza A/PR/8/34 virus overnight and then blocked with 10% FBS/coating buffer. Serially diluted (1:3) samples were plated and incubated for 2 h at 37°C. Each plate included a negative and known positive serum control. IgG Ab was detected using HRP biotinylated goat anti-mouse IgG (MP Biomedicals, Solon, OH) diluted 1:200 in PBS/10% FBS and incubated for 1 h at 37°C. Finally, 0.100 ml ABTS was added per well, and the resulting color change was quantified at 405 nm using an ELx808 Ultra Micro Plate Reader (Bio-Tek Instruments, Winooski, VT). Ab titers were determined by selecting the reciprocal of the last dilution two SDs above the mean OD of the negative serum control. The resulting titers were log-transformed to a geometric mean titer (GMT) for statistical analysis.

DTH response

Mice were lightly anesthetized by isoflurane (Abbott Laboratories, Abbott Park, IL) inhalation. Each mouse served as its own control; 20 μl saline or whole A/PR/8 was injected s.c. into each rear footpad. The thickness of each footpad was measured every 24 h for 4 d in a double-blinded manner (substance injected and treatment group), using a constant-loading micrometer(Mitutoyo, Aurora, IL).Ag-induced swelling was assessed by subtracting the thickness of the saline-injected foot from that of the Ag-injected foot each day (46,47).

Cell isolation

Mice were sacrificed via cervical dislocation. The apical lobe of each lung was flash-frozen in liquid nitrogen for PCR analysis, and the remaining lung was digested for 1 h on ice in HBSS and type I collagenase (Worthington, Lakewood, NJ). Spleens and lungs were pulverized using a Model 80 Biomaster Stomacher (Seward, Riverview, FL) in ice-cold HBSS. RBCs were lysed with buffer (0.16 M NH_4Cl, 10mM $KHCO_3$, 0.13 mM EDTA), and single-cell suspensions were filtered through a nylon 70-μm cell strainer (BD Biosciences, San Jose, CA). Lymph nodes were processed by mashing the nodes through a cell strainer and then RBCs were lysed in the same manner as the spleens. Bronchoalveolar lavage (BAL) fluid was collected by flushing the lungs through a tracheal cannula with a total of 3 ml PBS (Invitrogen, Grand Island, NY); protease inhibitor mixture tablets (Roche,

Indianapolis, IN) were added to PBS prior to lavage, per the manufacturer's instructions. Cell counts were determined using a Beckman Z2 Coulter Counter (Corixa, Seattle, WA), and cell concentrations were adjusted to 2.0×10^7 cells/ml for flow cytometry.

Flow cytometry

Specific lymphocyte subtypes were measured by immunofluorescent Ab staining and analysis using flow cytometry (FACSCalibur, BD Biosciences). Leukocyte subpopulations were identified and gated using forward- versus side-scatter characteristics. Cytotoxic T cells ($CD8^+$, $CD3^+$ cells) were identified using directly conjugated CD3e and CD8a (Ly-2) Abs. Influenza-specific $CD8^+$ cells ($NP_{366–74}Tetramer^+$, $CD8^+$ cells) were identified by gating on the $CD3^+/CD8^+$ lymphocyte population and then selecting the $CD8^+/NP_{366–74}{}^+$ events. An irrelevant tetramer for the HSV glycoprotein B 495–505 epitope (SSIEFARL) was used as a negative control for staining. The tetramer probes were conjugated by the National Institutes of Health Tetramer Facility at Emory University. The NP366–74 (influenza) and GB495–505 (HSV) peptides were synthesized by The Ohio State University Peptide Synthesis facility. The $NP_{366–74}$ probe consists of four peptide (ASNENMETM)/H-2Db complexes conjugated to a single commercially manufactured streptavidin-PE. All Abs were obtained from BD Biosciences (San Jose, CA), except for the FITC-conjugated anti-mouse CD127 Ab (eBioscience, San Diego, CA), and were matched with appropriate isotype controls. Briefly, 50 μl the single-cell suspension was incubated with anti-CD16/CD32 to block Fc receptors for 10 min at room temperature; titrated concentrations of fluorochrome-conjugated Abs were added for 45 min at 4°C. Samples were lysed and fixed with FACS lysing solution for 10 min, washed with FACS buffer, and read on the FACSCalibur (BD Biosciences); 100,000 events were acquired from each preparation. Appropriate compensation and isotype and negative controls were used to control for background and for instrument set-up. Results were analyzed using CellQuest software (BD Biosciences).

Intracellular staining

To enumerate the number of cytokine-producing cells, freshly isolated lung lymphocytes were processed as above to a single-cell suspension. Cells were then stimulated ex vivo with media alone, 10 μM $NP_{366–74}$ peptide (ASNENMETM), UV-inactivated influenza virus, or PMA (50 ng/ml) and ionomycin (500 ng/ml) for a 7-h incubation at 37°C with 5% CO_2. Golgi-Plug (BD Pharmingen) was added after 1 h. After the incubation, Fc receptors were blocked as above, and surface receptor staining was done with tetramer and fluorochrome-conjugated Abs. Cells were fixed and permeabilized, according to the manufacturer's instructions (BD Pharmingen), and then were stained with fluorochrome-conjugated anti–IFN-γAb, anti–IL-2 Ab, or the control isotype Ab (BD Pharmingen). Samples were read on a FACSCalibur, and the results were analyzed using CellQuest software.

Histopathology

At varying times postinfection, mice were sacrificed via cervical dislocation and perfused with PBS. The left lobe of the lung was inflated with 10% formalin, excised, fixed in 10% formalin, and processed for paraffin embedding. Thin sections (3 μm) were processed for H&E staining. Slides were observed on an Olympus BX41 microscope (Olympus America, Center Valley, PA) and evaluated by a pathologist.

Circulating corticosterone

Mice were decapitated, and trunk blood was collected into EDTA-coated tubes. Samples were collected after minimal manipulation at similar times of day. Plasma was separated,

and corticosterone was quantified using the DA Corticosterone RIA kit (MP Biomedicals, Solon, OH), according to manufacturer's instructions.

RNA extraction and real-time PCR

RNA was isolated from the apical lobe of the lung in TRIzol, according to manufacturer's instructions (Life Technologies, Carlsbad, CA). Reverse transcription and cDNA synthesis were carried out using a Promega kit (Madison, WI). Cytokine primer and probe sequences were developed with Primer Express Software from PE Biosystems (Foster City, CA), and the influenza A matrix (M1) protein primers and probe were based on a previously published sequence (48). The final concentration for the PCR was 900 nM for the primers and 100 nM for the probe. Cytokine and 18s probes were labeled at the 5′ end with the reporter dye FAM and at the 3′ end with the quencher dye TAMRA. Labeled probes were synthesized by PE Biosystems. Each plate included a positive control standard curve, with 1, 1:10, 1:100, and 1:1000 dilutions of a known sample with expression for the gene of interest. For analysis, the plate efficiency (E) was calculated from the slope of a dilution factor versus CT (cycle threshold) value curve for the dilutions using $E = 10(^{-1/\text{slope}}) - 1$. The modified CT value of each sample was calculated from gene expression and plate efficiency (eff) with the equation $CT_{gene}*\ln(1 + eff_{gene})$. This was subtracted from the sample's 18s expression modified as CT_{18s}-$\ln(1 + eff_{18s})$, resulting in the DCT(delta CT) value of the sample. The DCT of the control group, the uninfected day 0 MEM mice, was averaged to calculate the baseline DCT. This was subtracted from each sample's DCT to compute the delta DCT value, which represents the fold increase of gene expression over baseline. These are the values shown in the figures. The 95% confidence interval (CI) was calculated from the DCT values of each group. Nonoverlapping CIs are considered significantly different. To compare groups across multiple time points, individual delta DCT values were used for repeated-measures–ANOVA (RM-ANOVA).

Statistical analysis

DTH responses were compared by RM-ANOVA. Flow cytometry data were compared using a two-factor ANOVA, with individual *t* tests for post hoc analysis or when indicated by an a priori hypothesis. Real-time PCR data were treated as described above.

Results

SDR-MEM mice generated an enhanced DTH response

A DTH response was measured as an initial assessment of stress-induced alteration of MEM. For all memory studies, mice were exposed to SDR (SDR-MEM group) or were isolated from the stressor (MEM group). Thirty-six hours after the conclusion of the sixth SDR cycle, all animals were infected with influenza virus. For this portion of the study, the DTH reaction to influenza Ag challenge was measured in the footpad 6 wk after the primary infection. An s.c. footpad injection was used to install sterile saline in one rear footpad and whole A/PR8/34 virus in the other. The thickness of each footpad was measured at 24-h intervals by an investigator blinded to group and substance injected. The amount of swelling due to Ag was calculated by subtracting the saline-injected footpad thickness from the Ag-injected footpad thickness. Both groups showed a peak DTH response at the 48-h time point (Fig. 1*A*); however, the SDR-MEM group responded with a significantly greater DTH response overall ($p < 0.001$). Data shown are representative of four separate experiments with similar results. To confirm and extend these findings, IFN-γ production was assessed in $CD4^+$ T cells that were stimulated directly ex vivo with UV-inactivated A/PR/8/34 virus (UV-PR8). Results from whole spleen (Fig. 1*B*) or lung (Fig. 1*C*)single-cell suspensions cocultured with UV-PR8 indicate a significant upregulation ($p < 0.05$) in the number of IFN-γ–producing $CD4^+$ T cells found in the spleen or the lung of SDR-MEM mice at 6 wk after a

primary A/PR/8 infection. Stimulation with UV-PR8 produced a significant increase in the number of $IFN\gamma^+CD4^+$ T cells detected compared with media-alone stimulation. These ex vivo data confirmed the enhanced in vivo DTH response consistently observed in SDR-MEM mice.

Influenza viral M1 gene expression was attenuated in SDR-MEM mice during reinfection

The SDR-enhanced DTH response suggested that memory T cell responses were augmented. Viral mRNA was measured in the lungs to determine whether this memory T cell response correlated with a reduction in viral burden during an infectious rechallenge. To this end, a 16-HAU dose of A/PR/8/34 virus was administered to MEM and SDR-MEM groups. The apical lobe of the lung from days 0 (preinfection), 3, and 5 postreinfection was harvested and used for real-time RT-PCR analysis of influenza M1 gene expression. The influenza M1 gene codes for a protein that is part of the internal components of the virus and is detectable in infected tissue during viral replication (46). Expression of influenza M1 RNA detected by real-time PCR served as a surrogate marker of influenza virus replication in lung tissue. The fold increase/decrease data generated via real-time PCR were compared using 95% CIs to account for the nonparametric nature of these data; however, for clarity, the data are shown as group mean ± SEM. Nonoverlapping CIs at day 1 postchallenge (Fig. 2) indicate a significant reduction in M1 gene expression in the SDR-MEM group (11.3-fold less) compared with the MEM group. Gene expression in both memory groups had returned to baseline by day 3 postchallenge (Fig. 2). In four separate experiments, viral gene expression was terminated earlier in SDR-MEM mice. Additionally, SDR-MEM animals consistently allowed less overall viral gene expression during rechallenge, as evidenced by the low amount of virus mRNA detectable at the peak of the rechallenge in the apical lobe.

SDR-MEM mice had an attenuated corticosterone response during viral reinfection

An influenza viral infection in the mouse is known to activate the HPA axis, giving rise to elevated levels of circulating corticosterone (16,21). During an influenza rechallenge, MEM mice exhibited the expected increase in plasma corticosterone levels that temporally matched the real-time PCR curve for virus detected in lung tissue (Figs. 2, 3). In MEM mice, circulating corticosterone levels increased 4-fold, from 30 ng/ml during resting memory to 120 ng/ml at day 1 postinfection; they remained elevated throughout rechallenge at 80 ng/ml. In contrast, SDR-MEM mice had an attenuated corticosterone response to the viral rechallenge [$F(1,28) = 5.492$; $p < 0.05$; Fig. 3]. Although the systemic corticosterone increased in SDR-MEM mice from resting memory to day 1 postinfection, serum levels were half (60 ng/ml) that observed in MEM controls; by day 5 postinfection, corticosterone was significantly lower in SDRMEM mice compared with MEM controls. Rechallenge of memory mice resulted in HPA activation and corticosterone secretion, but this effect was diminished by exposure to SDR prior to the primary viral infection. Taken together with the viral clearance data, these results support a reduction in the severity of the viral infection in SDR-MEM mice following rechallenge.

Histological changes observed in SDR-MEM lungs include more cellular infiltrate during resting memory

Lung tissue was examined histologically to assess lung architecture, cellular infiltrate, and residual pathology during resting memory(30–60 d after a primary infection) and during influenza rechallenge. As expected, residual tissue damage from the primary infection was evident in MEM and SDR-MEM lungs and consisted of minimal areas of focal consolidation of alveoli with occasional associated degenerate and necrotic cellular debris. During resting memory, SDR-MEM mice had more mononuclear cells within the lung parenchyma. More damage was evident in pulmonary parenchymal tissues compared with nonstressed MEM controls (Fig. 4). Alveoli in SDR-MEM lungs were frequently

consolidated and filled with cellular and inflammatory debris, consisting predominantly of mononuclear cells with fewer neutrophils. SDR alone (data not shown) caused no long-term histological changes at 6 wk poststress, and sections looked similar to home cage control mice. During re-infection (data not shown), consistent intergroup differences were not evident, although both groups exhibited a clear cellular response to viral exposure. One to 2 mo after a primary influenza infection, during resting memory, more damage in the lung tissue was still present in SDR-MEM mice compared with the resolution observed in non-stressed MEM mice (Fig. 4).

SDR altered lung cellularity and environment during resting memory

The lung environment during resting memory, between 60 and 90 d postinfection, was assessed with respect to cytokine environment and resident memory cells. Although the known behavioral and physiological effects of SDR are generally gone by 30 d poststress, SDR-MEM mice had an altered lung cellularity and cytokine environment at 2–3 mo after SDR compared with nonstressed MEM controls (Fig. 5). In SDR-MEM mice, a significant increase in the lung IL-$7R_{HI}NP_{366}CD8^+$ memory phenotype population ($p < 0.05$) was noted in the absence of active infection (Fig. 5*A*). Real-time PCR indicated significant increases in mRNA expression for IL-2 and IFN-γ in SDR-MEM lung tissue at this time (Fig. 5*B*; comparison by 95% CIs). Finally, when lung $CD8^+$ T cells were stimulated ex vivo with NP366–74 peptide and stained intracellularly for IFN-γ production, flow cytometric analysis indicated that slightly more IFN-γ–producing $D^bNP_{366–74}$ $CD8^+$ T cells were isolated from SDR-MEM lungs (Fig. 5*C*). There was no change in the level of IFN-γ staining on a per-cell basis. Even well beyond the known time period of SDR-induced physiological changes, mice that were exposed to a primary influenza infection immediately after exposure to SDR maintained long-lasting changes in their lung environment and influenza-specific memory $CD8^+$ T cell population.

SDR increased the proportion of $D^bNP_{366–74}$ $CD8^+$ T cells to total $CD8^+$ T cells and increased the total number of $D^bNP_{366–74}$ $CD8^+$ T cells

After assessment of memory cell location and function during resting memory, mice were rechallenged with A/PR/8 to evaluate the impact of SDR on the recall function of the memory populations. Although H-$2D^b$–restricted mice respond to six known major epitopes of A/PR/8 virus, in these memory experiments, we focused on the major dominant epitope for memory responses: NP366–74 (49). The same paradigm was used as previously described, and mice were sampled at days 0 (resting memory), 3, and 5 post-infection. The staining intensity of NP366 tetramer on memory or effector $CD8^+$ T cells was not changed by exposure to SDR (Fig. 6*A*). SDR nearly doubled the proportion of lung $D^bNP_{366–74}$ $CD8^+$ T cells to total lung $CD8^+$ T cells detected during resting memory (Fig. 6*B*) and at the peak of the T cell response (day 5) to influenza reinfection (Fig. 6*C*). The frequency of the Ag-specific T cell population was assessed in immune repositories (spleen and mediastinal lymph nodes [MLNs]) and at the site of infection (lung and BAL). Prior to viral rechallenge, there was a significant ($p < 0.001$) increase in the number of lung $D^bNP_{366–74}$ $CD8^+$ T cells recovered from SDR-MEM animals compared with those from MEM mice (Fig. 7*A*). After reinfection with A/PR/8, the $D^bNP_{366–74}$ $CD8^+$ T cell population expanded rapidly and had doubled by day 3 post-infection in the MEM and SDR-MEM animals; however, because the SDR-MEM mice had a higher number of $D^bNP_{366–74}$ $CD8^+$ T cells in the lung parenchyma following the primary infection, this resulted in a larger lung-based expansion in the SDR-MEM group. At day 5 postchallenge, the SDR-MEM $D^bNP_{366–74}$ $CD8^+$ T cell population had expanded to its peak at 158 times its original size, and the MEM $D^bNP_{366–74}$ $CD8^+$ T cell population was 45 times its original size, as assessed during resting memory. Among the day 5 populations, there was a significant increase in virus-specific T cells detected in the lung ($p < 0.001$) and a 17-fold increase in virus-specific cells in the pooled BAL fluid of

SDR-MEM mice (Fig. 7*A*, 7*D*). In the spleen, an enlarged $D^bNP_{366–74}$ $CD8^+$ T cell population was consistently found in SDR-MEM mice ($p < 0.05$) but only during the resting memory phase and not during reinfection. Events detected in the MLN were equivalent during resting memory and were not significantly different throughout the recall response (Fig. 7*C*). Interestingly, the largest change in the MLN $D^bNP_{366–74}$ $CD8^+$ T cell population occurred on day 5 postinfection in the SDR-MEM group. The difference in the number of MLN cells detected did not reach statistical significance; however, only 3% of all CD8 T cells detected at day 5 in the MEM MLN were $NP_{366–74}$ $CD8^+$ T cells, whereas 17% of all CD8 T cells in the SDR-MEM MLN were $NP_{366–74}$ $CD8^+$ T cells. The number of whole $CD8^+$ T cells in each compartment is shown in Supplemental Fig. 1.

SDR increased the size of the lung $IL7R_{HI}$ $D^bNP_{366–74}$ $CD8^+$ T cell population

Effector cells were costained for IL-7Rα (Fig. 8). Prior to re-infection, no significant differences were detected in $IL7R_{HI}D^b$ $NP_{366–74}$ $CD8^+$ T cell population in the spleen between MEM and SDR-MEM mice, despite the significantly increased $D^bNP_{366–74}$ $CD8^+$ T cell population found within the spleen ($p < 0.05$). However, in the lung parenchyma, significantly more $IL7R_{HI}D^b$ $NP_{366–74}$ $CD8^+$ T cells were detected prior to infection and at day 5 of the reinfection ($p < 0.005$; individual *t* test), which culminated as a significant enhancement throughout the time course (two-factor ANOVA, $p < 0.0001$ overall). These data indicate that the enlarged memory $CD8^+$ T cell population was localized to the lung parenchyma, rather than residing primarily in the spleen or other immune repositories.

SDR had a differential effect on the cytokine profile during reinfection

The cytokine environment of the lung was sampled during the reinfection using real-time PCR. The expression of IL-2 remained significantly elevated prior to and during rechallenge in the lung tissue, and it ranged from a 2.02- to a 3.33-fold increase in SDRMEM mice compared with the MEM group ($p < 0.05$ by 95% CI and ANOVA). As noted earlier, the expression of IFN-γ was significantly increased at various times during resting memory, with an average increase of 1.77-fold. However, no statistically significant enhancement was seen in lung IFN-γ expression during rechallenge, although there was a trend toward increased mRNA expression (data not shown).

Functionally, when IFN-γ production was assessed via flow cytometry, using ex vivo peptide stimulation and intracellular staining during rechallenge, we found no changes in the geometric mean fluorescence intensity between the groups, nor was there a significant change in the percentage of IFN-γ–producing D^b $NP_{366–74}$ $CD8^+$ T cells detected in the MEM or SDR-MEM groups (data not shown). As discussed above, there was a larger number of IFN-γ–producing $D^bNP_{366–74}$ $CD8^+$ T cells present in the lung during resting memory (Fig. 5*C*); however, this change did not reach statistical significance or carry over into the rechallenge.

SDR positively impacted cell-mediated protection but not Ab-mediated protection

The anti-influenza serum IgG titers were measured during resting memory and throughout the homologous prime-challenge experiments (Fig. 9). The titers are shown as 95% CIs of the GMT at each day postchallenge. During resting memory, SDR-MEM mice had a >4-fold decrease in raw titer, and the 95% CI for the GMT was discordant from that of the SDR-MEM group, as confirmed by a two-sample *t* test ($p = 0.007$), which strongly supports a significant attenuation of the serum anti-influenza whole IgG Ab titer in the SDR-MEM group. However, this difference was abrogated during homologous A/PR/8/34 rechallenge, and no intergroup differences were noted through this period.

To clarify the role of cell-mediated protection versus Ab-mediated protection, a heterologous prime-challenge system was used to define the role of Ab-mediated protection during the rechallenge infection. Influenza X-31, an H3N2 influenza virus that shares six internal proteins and a class I immunodominance hierarchy with A/PR/8/34, was used to prime mice with an intranasal infection without generating anti-hemagglutinin or anti-neuraminidase Abs to A/PR/8/34, the virus that was then used for the challenge infection. The data are presented in Fig. 10. Interestingly, no augmentation of the $D^bNP_{366–74}$ $CD8^+$ T cell population was seen in lung tissue during resting memory or challenge with the A/PR/8 virus (Fig. 10*A*). However, at day 5 postchallenge, the number of D^b $NP_{366–74}$ $CD8^+$ T cells in the pooled BAL sample ($n = 6$ per group) was doubled in the SDR-MEM mice (Fig. 10*D*). In the spleen, significant increases in the SDR-MEM $D^bNP_{366–74}$ $CD8^+$ T cell population were seen at each day throughout heterologous influenza infection (Fig. 10*B*; $p < 0.05$). When lung cell function was probed, using ex vivo stimulation with NP366–74 peptide and stained for intracellular IFN-γ production, there was a significant increase in the number of IFN-γ–producing$NP_{366–74}$ cells isolated from SDR-MEM lungs compared with MEM lung cells during resting memory but not during A/PR/8 challenge (Supplemental Fig. 2*A*). However, no difference was seen in viral clearance, as assessed by 50% tissue culture infectious dose using whole lung homogenates, or in viral gene expression, as assessed by influenza M1 gene expression, in the heterologous prime-challenge system (data not shown). Lung cytokine gene expression in the heterologous prime-challenge system was analogous to that in the homologous A/PR/8 system; however, the pattern differed (Supplemental Fig. 2*B*) throughout the course of the rechallenge. A significant increase in IL-2 and TNF-α was evident only on day 5 postchallenge ($p < 0.05$) in SDR-MEM mice.

Discussion

The present study evaluated the effect of social stress prior to a sublethal primary influenza viral infection on the subsequent virus-specific T cell memory in male mice. Studies demonstrated that SDR prior to the primary infection increased the frequency of memory $D^bNP_{366–74}$ $CD8^+$ T cells and the corresponding recall response, without changing the TCR expression or effector function on a per-cell basis. The enlarged memory population was primarily localized to the lung parenchyma; however, more epitope-specific $CD8^+$ T cells, relative to nonstressed controls, were also found in the spleen during the resting memory phase in SDRMEM mice. Enhanced expression of IL-2 and IFN-γ mRNA, cytokines that support homeostatic proliferation and T cell stimulation, was detected in the lungs. Enhanced production of these cytokines would sustain an enlarged memory $CD8^+$ T cell population within the lung and support an expeditious response to a second encounter with influenza virus. Finally, these combined immunologic changes seem to functionally benefit SDR-MEM mice, because they were able to terminate viral gene expression earlier than MEM mice when rechallenged with the A/PR/8 virus.

The role of Ab versus T cells in this system was further defined using an X-31 influenza prime/PR8 challenge system. SDR-MEM mice that were primed with X-31 influenza had significantly enhanced numbers of splenic $D^bNP_{366–74}$ $CD8^+$ T cells during resting memory and rechallenge; however, cell number in the lung parenchyma was unchanged between MEM and SDR-MEM mice. The virulence of the X-31 virus is attenuated compared with the A/PR/8 virus and is less likely to cause a severe infection. The reduced virulence of the X-31 virus may account for differences seen in localization of the $D^bNP_{366–74}$ $CD8^+$ T cells. Alternatively, changes after X-31 priming may have been too small to detect in lung tissue during resting memory. When lung cells were stimulated ex vivo with NP366 peptide, a significant increase was detected in the number of IFN-γ–producing $CD8^+$ T cells from SDR-MEM mice. This suggests that SDR enhanced the memory T cell population after X-31 primary infection; however, the $CD8^+$ T cell population seems to be differentially

localized, depending on the virus used for the primary infection. Two reports and one meta-analysis from vaccination studies done in human populations suggest that psychological stress alters the immune response to H1N1 influenza strains, but it has less to no effect on the response to H3N2 strains of influenza (50–52). These reports do not completely align with the present data and may be more related to existing heterosubtypic immunity within the human population; however, they do confirm that stress is known to differentially affect the antiviral immune response to different subtypes of the same virus. Chronic stress in human populations is known to depress the Ab response to antiviral vaccinations, presumably through HPA axis regulation (53–55). This precedent was further established in SDR-like models of nonchronic murine stress (56). The role of anti-influenza Ab in this system is not negligible; however, it seems to be primarily related to altered localization of the memory T cell population. More research is needed to precisely tease out the role of virus subtype and humoral immunity in the SDR system.

IL-7R (CD127) binds IL-7 and allows cells to receive environmental antiapoptotic and survival signals. It is a candidate phenotypic marker for memory $CD8^+$ T cells (40,41). The promoter region of the IL-7R gene contains a GC response element (57). Franchimont et al. (57) suggested that upregulation of IL-7R on $CD8^+$ T cells via GC signaling was a mechanism through which GCs could promote the function and survival of human memory $CD8^+$ T cells. SDR is known to render $CD11b^+$ monocytes resistant to GCs after SDR, but similar parameters have not been evaluated in the $CD8^+$ T cell population (42). Immediately following an SDR cycle, SDR mice have increased levels of circulating corticosterone; however, this returns to baseline within 12 h and remains at a normal level 36 h after the final cycle of SDR—the time point at which the primary influenza viral infection was started during these studies. This suggests that SDR-induced corticosterone could influence the fate decision of the $CD8^+$ T cells. However, the SDR cycles are completed prior to the experimental viral infection and initial $CD8^+$ T cell activation. Studies need to be done in this model system to investigate any direct signaling between the CD127 gene and SDR-induced stress mediators. When we stained resting memory and effector memory $D^bNP_{366–74}$ $CD8^+$ T cells for CD127, there was a significantly larger population in the lung prior to reinfection and at day 5 of the challenge. Thus, it is possible that the SDR-induced changes in the memory $D^bNP_{366–74}$ $CD8^+$ T cell population primarily affected the memory cells retained within the lung parenchyma. Upregulation of CD127 on $CD8^+$ T cells is a potential mechanism through which more activated $CD8^+$ T cells could survive beyond resolution of a primary influenza infection.

During reinfection, the number of memory $D^bNP_{366–74}$ $CD8^+$ T cell was increased in the SDR-MEM mice; however, the functional capabilities of the cells may be the more important parameter for host protection against the virus. After the viral rechallenge, the SDR-MEM mice allowed less overall viral gene expression in their lung tissue compared with MEM controls, and they terminated viral gene expression earlier in lung tissue. When IFN-γ production by the $D^bNP_{366–74}$ $CD8^+$ T cells was examined, no differences were noted on a per-cell basis between MEM and SDR-MEM cells. The changes observed in viral clearance were not a result of altered function in the SDR-MEM $D^bNP_{366–74}$ $CD8^+$ T cells but rather were due to the increased frequency of effector cells. Cytokine gene expression in the lung tissue corresponded neatly to the changes observed in the $CD8^+$ T cell population. Specifically, there was an increased expression of the effector cytokine IFN-γ prior to and at day 1 postchallenge in SDR-MEM animals, when influenza virus was also present, and lung-based $D^bNP_{366–74}$ $CD8^+$ memory cells may have been stimulated. Although a balance between lung cytokines TNF-α and IL-10 was reported as important for mediating lung damage versus protection, no consistent trend was seen in these studies for IL-10 gene expression in the lung (58,59). TNF-α was up-regulated in SDR-MEM mice during resting memory in four experiments, and given the level of residual tissue damage observed in the

lungs at this time, it may have played a role in retarding tissue repair. IL-2 gene expression in lung tissue was enhanced in the SDR-MEM group prior to and throughout the rechallenge. The role of IL-2 on $CD8^+$ T cells during homeostatic proliferation or a recall response is not well understood. Studies suggest that IL-2 supports the homeostatic proliferation of $CD8^+$ T cells, and more of this cytokine could enhance expansion and function of the $D^bNP_{366–74}$ $CD8^+$ T cell population during a recall response (60,61). Conflicting studies suggest that IL-2 increases the size of the memory pool only when present prior to $CD8^+$ T cell stimulation; however, when present during resting memory, it inhibits the proliferation of memory $CD8^+$ T cells (62). In the current study, IL-2 mRNA was first detectable in lung tissue of SDR-MEM mice during resting memory. Although the precise function of IL-2 upregulation in this model is not clear, Swain et al. (2) recently reported that memory $CD4^+$ T cells reacquire the ability to produce IL-2. The DTH studies that we performed in the SDR model suggest that because a large portion of the DTH response at 48 h is composed of memory $CD4^+$ T cells, this population is likely enlarged in SDR-MEM mice. In lung tissue, as assessed during resting memory, the $CD4^+$ T cell seemed to be a key source of IL-2 when stimulated with UV-PR8. Further research is needed to determine the role of IL-2 in this system.

The immune response plays an important role in the induction of lung pathology during an influenza infection. It is well-established that a vigorous antiviral immune response can be more detrimental to the host than the viral infection itself (63). The lung is an organ in which function is highly dependent on architecture. In this model, increased histopathology was observed after resolution of the primary infection in SDR-MEM mice. Although we did not assess lung function during resting memory or reinfection, residual inflammatory infiltrate and partial consolidation is not likely of benefit to the host. The experience of SDR in this model is not universally advantageous to the antiviral immune response. However, given the current thrust toward the development of T cell-targeted vaccines to elicit broader-spectrum protection against rapidly drifting influenza viruses, further investigation of the mechanisms by which social stress increases T cell memory responses may be warranted (64).

Human studies have addressed the issue of potential advantageous effects of stress on the adaptive immune system. Through careful design and analysis, two studies in humans showed that short-term physical and psychological stressors were able to enhance the adaptive cellular immune response by mobilizing $CD8^+$ T cells and enhancing the immune response to vaccination (65,66). In a 2006 randomized clinical trial, Edwards et al. (66) used an acute exercise stressor as a behavioral adjuvant prior to the administration of influenza vaccine in young adults. They found that the resulting anti-influenza Ab response was increased in females, whereas males had an enhanced IFN-γ response. Memory $CD8^+$ T cells were mobilized into the blood stream and directed for migration into lymphoid tissues. Also in 2006, Atanackovic et al. (65) used an acute psychological stressor with no physical component and found that exposure to the stress task redistributed naive and memory $CD8^+$ T cells in humans. Finally, a recent study used a rhesus macaque model to demonstrate that exposure to chronic social stress can persistently desensitize cells of the immune system to normal physiologic regulation by endogenous GCs, similar to the phenomenon seen in the SDR murine model of social stress (67). These studies imply that psychosocial stress could have similar potential in humans and may widen the implications of the current study.

In the SDR model, augmentation of T cell memory takes place during the primary infection or shortly thereafter, because enhanced memory parameters are in place after resolution of the primary infection. It is recognized that the shape of T cell memory is patterned during the primary response (68). We hypothesize that the changes we observed were due to indirect effects of SDR on T cells, induced by altered cytokine expression profiles and

associated changes in the dendritic cell (DC) populations. Psychological stress was shown to act as an adjuvant for mouse DCs, and two studies showed that stress may upregulate activation markers on DCs or alter their migration pattern (69,70). Changes observed in the localization of memory $CD8^+$ T cells further suggest that SDR may alter the expression of adhesion molecules within the lung parenchyma or on memory $CD8^+$ T cells themselves. Additional immunohistochemical studies are needed to determine the effect of SDR on the lung microenvironment immediately after SDR and during a primary influenza infection. Alternatively, SDR may have altered the regulation of the contraction phase in a manner that would have left a larger memory T cell pool intact. This could include direct effects on the $CD8^+$ T cells, such as GC-induced upregulation of CD127 or enhanced secretion of anti-apoptotic factors.

Overall, the experience of SDR prior to a primary influenza viral infection imparted an advantage to the development and maintenance of murine MEM in the form of a larger $NP_{366–74}$ $CD8^+$ T cell population, with greater expansion and/or trafficking upon rechallenge. The precise neuroendocrine factor(s) responsible for the induction of enhanced MEM by social stress remain to be elucidated. Understanding how social stress alters the immune response to a viral challenge is pertinent to the development of more effective vaccination strategies, as well as for comprehending ways in which stressors interact clinically with important viral infections and antiviral vaccination.

Supplementary Material

Refer to Web version on PubMed Central for supplementary material.

Acknowledgments

We thank Mark Hanke, Marta Strembitsky, Jacqueline Verity, and Amy Hufnagle for excellent technical assistance.

This work was supported by grants from the National Institute of Mental Health (RO1 MH46801-17) and the National Institute of Dental and Craniofacial Research (T32DE014320-08 to J.F.S. and F30 DE17068-03 to J.W.M).

Abbreviations used in this paper

BAL	bronchoalveolar lavage
CI	confidence interval
CT	cycle threshold
DC	dendritic cell
DCT	delta CT
DTH	delayed-type hypersensitivity
GC	glucocorticoid
GMT	geometric mean titer
HAU	hemagglutinating unit
HPA	hypothalamic-pituitary-adrenal
MEM	immunological memory
MFI	mean fluorescence intensity
MLN	mediastinal lymph node

RM-ANOVA	repeated-measures–ANOVA
SDR	social disruption stress
UV-PR8	UV-inactivated A/PR/8/34 virus

References

1. Nicholson KG, Wood JM, Zambon M. Influenza. Lancet. 2003; 362:1733–1745. [PubMed: 14643124]
2. Swain SL, Agrewala JN, Brown DM, Jelley-Gibbs DM, Golech S, Huston G, Jones SC, Kamperschroer C, Lee WH, McKinstry KK, et al. CD4+ T-cell memory: generation and multi-faceted roles for CD4+ T cells in protective immunity to influenza. Immunol. Rev. 2006; 211:8–22. [PubMed: 16824113]
3. Gourley TS, Wherry EJ, Masopust D, Ahmed R. Generation and maintenance of immunological memory. Semin. Immunol. 2004; 16:323–333. [PubMed: 15528077]
4. Kohlmeier JE, Miller SC, Woodland DL. Cutting edge: antigen is not required for the activation and maintenance of virus-specific memory CD8+ T cells in the lung airways. J. Immunol. 2007; 178:4721–4725. [PubMed: 17404250]
5. Wakim LM, Gebhardt T, Heath WR, Carbone FR. Cutting edge: local recall responses by memory T cells newly recruited to peripheral non-lymphoid tissues. J. Immunol. 2008; 181:5837–5841. [PubMed: 18941171]
6. Wakim LM, Waithman J, van Rooijen N, Heath WR, Carbone FR. Dendritic cell-induced memory T cell activation in nonlymphoid tissues. Science. 2008; 319:198–202. [PubMed: 18187654]
7. Woodland DL, Kohlmeier JE. Migration, maintenance and recall of memory T cells in peripheral tissues. Nat. Rev. Immunol. 2009; 9:153–161. [PubMed: 19240755]
8. Masopust D, Vezys V, Marzo AL, Lefrançois L. Preferential localization of effector memory cells in nonlymphoid tissue. Science. 2001; 291:2413–2417. [PubMed: 11264538]
9. Hogan RJ, Usherwood EJ, Zhong W, Roberts AA, Dutton RW, Harmsen AG, Woodland DL. Activated antigen-specific CD8+ T cells persist in the lungs following recovery from respiratory virus infections. J. Immunol. 2001; 166:1813–1822. [PubMed: 11160228]
10. Calcagni E, Elenkov I. Stress system activity, innate and T helper cytokines, and susceptibility to immune-related diseases. Ann. N. Y. Acad. Sci. 2006; 1069:62–76. [PubMed: 16855135]
11. Kiecolt-Glaser JK, Marucha PT, Malarkey WB, Mercado AM, Glaser R. Slowing of wound healing by psychological stress. Lancet. 1995; 346:1194–1196. [PubMed: 7475659]
12. Padgett DA, Glaser R. How stress influences the immune response. Trends Immunol. 2003; 24:444–448. [PubMed: 12909458]
13. Sanders VM, Kohm AP. Sympathetic nervous system interaction with the immune system. Int. Rev. Neurobiol. 2002; 52:17–41. [PubMed: 12498099]
14. Webster JI, Sternberg EM. Role of the hypothalamic-pituitary-adrenal axis, glucocorticoids and glucocorticoid receptors in toxic sequelae of exposure to bacterial and viral products. J. Endocrinol. 2004; 181:207–221. [PubMed: 15128270]
15. Truckenmiller ME, Princiotta MF, Norbury CC, Bonneau RH. Corticosterone impairs MHC class I antigen presentation by dendritic cells via reduction of peptide generation. J. Neuroimmunol. 2005; 160:48–60. [PubMed: 15710457]
16. Hermann G, Beck FM, Sheridan JF. Stress-induced glucocorticoid response modulates mononuclear cell trafficking during an experimental influenza viral infection. J. Neuroimmunol. 1995; 56:179–186. [PubMed: 7860713]
17. Felten DL, Felten SY, Bellinger DL, Carlson SL, Ackerman KD, Madden KS, Olschowki JA, Livnat S. Noradrenergic sympathetic neural interactions with the immune system: structure and function. Immunol. Rev. 1987; 100:225–260. [PubMed: 3326822]

18. Felten SY, Madden KS, Bellinger DL, Kruszewska B, Moynihan JA, Felten DL. The role of the sympathetic nervous system in the modulation of immune responses. Adv. Pharmacol. 1997; 42:583–587. [PubMed: 9327969]
19. Kohm AP, Sanders VM. Norepinephrine and beta 2-adrenergic receptor stimulation regulate CD4+ T and B lymphocyte function in vitro and in vivo. Pharmacol. Rev. 2001; 53:487–525. [PubMed: 11734616]
20. Baile EM. The anatomy and physiology of the bronchial circulation. J. Aerosol Med. 1996; 9:1–6. [PubMed: 10160199]
21. Dunn AJ, Powell ML, Meitin C, Small PA Jr. Virus infection as a stressor: influenza virus elevates plasma concentrations of corticosterone, and brain concentrations of MHPG and tryptophan. Physiol. Behav. 1989; 45:591–594. [PubMed: 2756050]
22. Alleva E, Santucci D. Psychosocial vs. “physical” stress situations in rodents and humans: role of neurotrophins. Physiol. Behav. 2001; 73:313–320. [PubMed: 11438356]
23. Moynihan JA, Ader R. Psychoneuroimmunology: animal models of disease. Psychosom. Med. 1996; 58:546–558. [PubMed: 8948003]
24. Sheridan JF, Padgett DA, Avitsur R, Marucha PT. Experimental models of stress and wound healing. World J. Surg. 2004; 28:327–330. [PubMed: 14961184]
25. Avitsur R, Stark JL, Sheridan JF. Social stress induces glucocorticoid resistance in subordinate animals. Horm. Behav. 2001; 39:247–257. [PubMed: 11374910]
26. Bailey MT, Avitsur R, Engler H, Padgett DA, Sheridan JF. Physical defeat reduces the sensitivity of murine splenocytes to the suppressive effects of corticosterone. Brain Behav. Immun. 2004; 18:416–424. [PubMed: 15265534]
27. Kinsey SG, Bailey MT, Sheridan JF, Padgett DA, Avitsur R. Repeated social defeat causes increased anxiety-like behavior and alters splenocyte function in C57BL/6 and CD-1 mice. Brain Behav. Immun. 2007; 21:458–466. [PubMed: 17178210]
28. Avitsur R, Stark JL, Dhabhar FS, Sheridan JF. Social stress alters splenocyte phenotype and function. J. Neuroimmunol. 2002; 132:66–71. [PubMed: 12417435]
29. Avitsur R, Kavelaars A, Heijnen C, Sheridan JF. Social stress and the regulation of tumor necrosis factor-alpha secretion. Brain Behav. Immun. 2005; 19:311–317. [PubMed: 15944070]
30. Stark JL, Avitsur R, Hunzeker J, Padgett DA, Sheridan JF. Interleukin-6 and the development of social disruption-induced glucocorticoid resistance. J. Neuroimmunol. 2002; 124:9–15. [PubMed: 11958817]
31. Bailey MT, Engler H, Powell ND, Padgett DA, Sheridan JF. Repeated social defeat increases the bactericidal activity of splenic macrophages through a Toll-like receptor-dependent pathway. Am. J. Physiol. Regul. Integr. Comp. Physiol. 2007; 293:R1180–R1190. [PubMed: 17596326]
32. Avitsur R, Stark JL, Dhabhar FS, Padgett DA, Sheridan JF. Social disruption-induced glucocorticoid resistance: kinetics and site specificity. J. Neuroimmunol. 2002; 124:54–61. [PubMed: 11958822]
33. Badovinac VP, Tvinnereim AR, Harty JT. Regulation of antigen-specific CD8+ T cell homeostasis by perforin and interferon-gamma. Science. 2000; 290:1354–1358. [PubMed: 11082062]
34. Haring JS, Corbin GA, Harty JT. Dynamic regulation of IFN-gamma signaling in antigen-specific CD8+ T cells responding to infection. J. Immunol. 2005; 174:6791–6802. [PubMed: 15905520]
35. Kolumam GA, Thomas S, Thompson LJ, Sprent J, Murali-Krishna K. Type I interferons act directly on CD8 T cells to allow clonal expansion and memory formation in response to viral infection. J. Exp. Med. 2005; 202:637–650. [PubMed: 16129706]
36. Whitmire JK, Benning N, Whitton JL. Cutting edge: early IFN-gamma signaling directly enhances primary antiviral CD4+ T cell responses. J. Immunol. 2005; 175:5624–5628. [PubMed: 16237051]
37. Whitmire JK, Tan JT, Whitton JL. Interferon-gamma acts directly on CD8+ T cells to increase their abundance during virus infection. J. Exp. Med. 2005; 201:1053–1059. [PubMed: 15809350]
38. Hou S, Hyland L, Ryan KW, Portner A, Doherty PC. Virus-specific CD8+ T-cell memory determined by clonal burst size. Nature. 1994; 369:652–654. [PubMed: 7516039]
39. Belz GT, Xie W, Doherty PC. Diversity of epitope and cytokine profiles for primary and secondary influenza a virus-specific CD8+ T cell responses. J. Immunol. 2001; 166:4627–4633. [PubMed: 11254721]

40. Huster KM, Busch V, Schiemann M, Linkemann K, Kerksiek KM, Wagner H, Busch DH. Selective expression of IL-7 receptor on memory T cells identifies early CD40L-dependent generation of distinct CD8+ memory T cell subsets. Proc. Natl. Acad. Sci. USA. 2004; 101:5610–5615. [PubMed: 15044705]
41. Kaech SM, Tan JT, Wherry EJ, Konieczny BT, Surh CD, Ahmed R. Selective expression of the interleukin 7 receptor identifies effector CD8 T cells that give rise to long-lived memory cells. Nat. Immunol. 2003; 4:1191–1198. [PubMed: 14625547]
42. Stark JL, Avitsur R, Padgett DA, Campbell KA, Beck FM, Sheridan JF. Social stress induces glucocorticoid resistance in macrophages. Am. J. Physiol. Regul. Integr. Comp. Physiol. 2001; 280:R1799–R1805. [PubMed: 11353685]
43. Avitsur R, Kinsey SG, Bidor K, Bailey MT, Padgett DA, Sheridan JF. Subordinate social status modulates the vulnerability to the immunological effects of social stress. Psychoneuroendocrinology. 2007; 32:1097–1105. [PubMed: 17954013]
44. Padgett DA, Sheridan JF. Androstenediol (AED) prevents neuroendocrine-mediated suppression of the immune response to an influenza viral infection. J. Neuroimmunol. 1999; 98:121–129. [PubMed: 10430045]
45. Daly KP, Nguyen DL, Woodland, Blackman MA. Immunodominance of major histocompatibility complex class I-restricted influenza virus epitopes can be influenced by the T-cell receptor repertoire. J. Virol. 1995; 69:7416–7422. [PubMed: 7494246]
46. Luo, Y.; Dorf, ME. Curr. Protoc. Immunol. Vol. 6. John Wiley & Sons: Hoboken, NJ.; 1993. In-Vivo Assays for Lymphocyte Function; p. 4.5.1-4.5.5.
47. Sunday ME, Weinberger JZ, Benacerraf B, Dorf ME. Hapten-specific T cell responses to 4-hydroxy-3-nitrophenyl acetyl. J. Immunol. 1980; 125:1601–1605. [PubMed: 6967910]
48. van Elden LJ, Nijhuis M, Schipper P, Schuurman R, van Loon AM. Simultaneous detection of influenza viruses A and B using real-time quantitative PCR. J. Clin. Microbiol. 2001; 39:196–200. [PubMed: 11136770]
49. Doherty PC, Turner SJ, Webby RG, Thomas PG. Influenza and the challenge for immunology. Nat. Immunol. 2006; 7:449–455. [PubMed: 16622432]
50. Pedersen AF, Zachariae R, Bovbjerg DH. Psychological stress and antibody response to influenza vaccination: a meta-analysis. Brain Behav. Immun. 2009; 23:427–433. [PubMed: 19486657]
51. Burns VE, Carroll D, Drayson M, Whitham M, Ring C. Life events, perceived stress and antibody response to influenza vaccination in young, healthy adults. J. Psychosom. Res. 2003; 55:569–572. [PubMed: 14642989]
52. Pressman SD, Cohen S, Miller GE, Barkin A, Rabin BS, Treanor JJ. Loneliness, social network size, and immune response to influenza vaccination in college freshmen. Health Psychol. 2005; 24:297–306. [PubMed: 15898866]
53. Glaser R, Kiecolt-Glaser JK, Malarkey WB, Sheridan JF. The influence of psychological stress on the immune response to vaccines. Ann. N. Y. Acad. Sci. 1998; 840:649–655. [PubMed: 9629291]
54. Kiecolt-Glaser JK, Glaser R, Gravenstein S, Malarkey WB, Sheridan J. Chronic stress alters the immune response to influenza virus vaccine in older adults. Proc. Natl. Acad. Sci. USA. 1996; 93:3043–3047. [PubMed: 8610165]
55. Vedhara K, Cox NK, Wilcock GK, Perks P, Hunt M, Anderson S, Lightman SL, Shanks NM. Chronic stress in elderly carers of dementia patients and antibody response to influenza vaccination. Lancet. 1999; 353:627–631. [PubMed: 10030328]
56. de Groot J, Boersma WJ, Scholten JW, Koolhaas JM. Social stress in male mice impairs long-term antiviral immunity selectively in wounded subjects. Physiol. Behav. 2002; 75:277–285. [PubMed: 11897253]
57. Franchimont D, Galon J, Vacchio MS, Fan S, Visconti R, Frucht DM, Geenen V, Chrousos GP, Ashwell JD, O'Shea JJ. Positive effects of glucocorticoids on T cell function by up-regulation of IL-7 receptor alpha. J. Immunol. 2002; 168:2212–2218. [PubMed: 11859107]
58. Sun J, Madan R, Karp CL, Braciale TJ. Effector T cells control lung inflammation during acute influenza virus infection by producing IL-10. Nat. Med. 2009; 15:277–284. [PubMed: 19234462]

59. Hackett TL, Holloway R, Holgate ST, Warner JA. Dynamics of pro-inflammatory and anti-inflammatory cytokine release during acute inflammation in chronic obstructive pulmonary disease: an ex vivo study. Respir. Res. 2008; 9:47. [PubMed: 18510721]
60. Ke Y, Ma H, Kapp JA. Antigen is required for the activation of effector activities, whereas interleukin 2 is required for the maintenance of memory in ovalbumin-specific, CD8+ cytotoxic T lymphocytes. J. Exp. Med. 1998; 187:49–57. [PubMed: 9419210]
61. Saparov A, Wagner FH, Zheng R, Oliver JR, Maeda H, Hockett RD, Weaver CT. Interleukin-2 expression by a subpopulation of primary T cells is linked to enhanced memory/effector function. Immunity. 1999; 11:271–280. [PubMed: 10514005]
62. Dai Z, Konieczny BT, Lakkis FG. The dual role of IL-2 in the generation and maintenance of CD8+ memory T cells. J. Immunol. 2000; 165:3031–3036. [PubMed: 10975812]
63. La Gruta NL, Kedzierska K, Stambas J, Doherty PC. A question of self-preservation: immunopathology in influenza virus infection. Immunol. Cell Biol. 2007; 85:85–92. [PubMed: 17213831]
64. Thomas PG, Keating R, Hulse-Post DJ, Doherty PC. Cell-mediated protection in influenza infection. Emerg. Infect. Dis. 2006; 12:48–54. [PubMed: 16494717]
65. Atanackovic D, Schnee B, Schuch G, Faltz C, Schulze J, Weber CS, Schafhausen P, Bartels K, Bokemeyer C, Brunner-Weinzierl MC, Deter HC. Acute psychological stress alerts the adaptive immune response: stress-induced mobilization of effector T cells. J. Neuroimmunol. 2006; 176:141–152. [PubMed: 16712956]
66. Edwards KM, Burns VE, Allen LM, McPhee JS, Bosch JA, Carroll D, Drayson M, Ring C. Eccentric exercise as an adjuvant to influenza vaccination in humans. Brain Behav. Immun. 2007; 21:209–217. [PubMed: 16824730]
67. Cole SW, Mendoza SP, Capitanio JP. Social stress desensitizes lymphocytes to regulation by endogenous glucocorticoids: insights from in vivo cell trafficking dynamics in rhesus macaques. Psychosom. Med. 2009; 71:591–597. [PubMed: 19553289]
68. Masopust D, Kaech SM, Wherry EJ, Ahmed R. The role of programming in memory T-cell development. Curr. Opin. Immunol. 2004; 16:217–225. [PubMed: 15023416]
69. Saint-Mezard P, Chavagnac C, Bosset S, Ionescu M, Peyron E, Kaiserlian D, Nicolas JF, Bérard. F. Psychological stress exerts an adjuvant effect on skin dendritic cell functions in vivo. J. Immunol. 2003; 171:4073–4080. [PubMed: 14530328]
70. Powell ND, Bailey MT, Mays JW, Stiner-Jones LM, Hanke ML, Padgett DA, Sheridan JF. Repeated social defeat activates dendritic cells and enhances Toll-like receptor dependent cytokine secretion. Brain Behav. Immun. 2009; 23:225–231. [PubMed: 18848983]

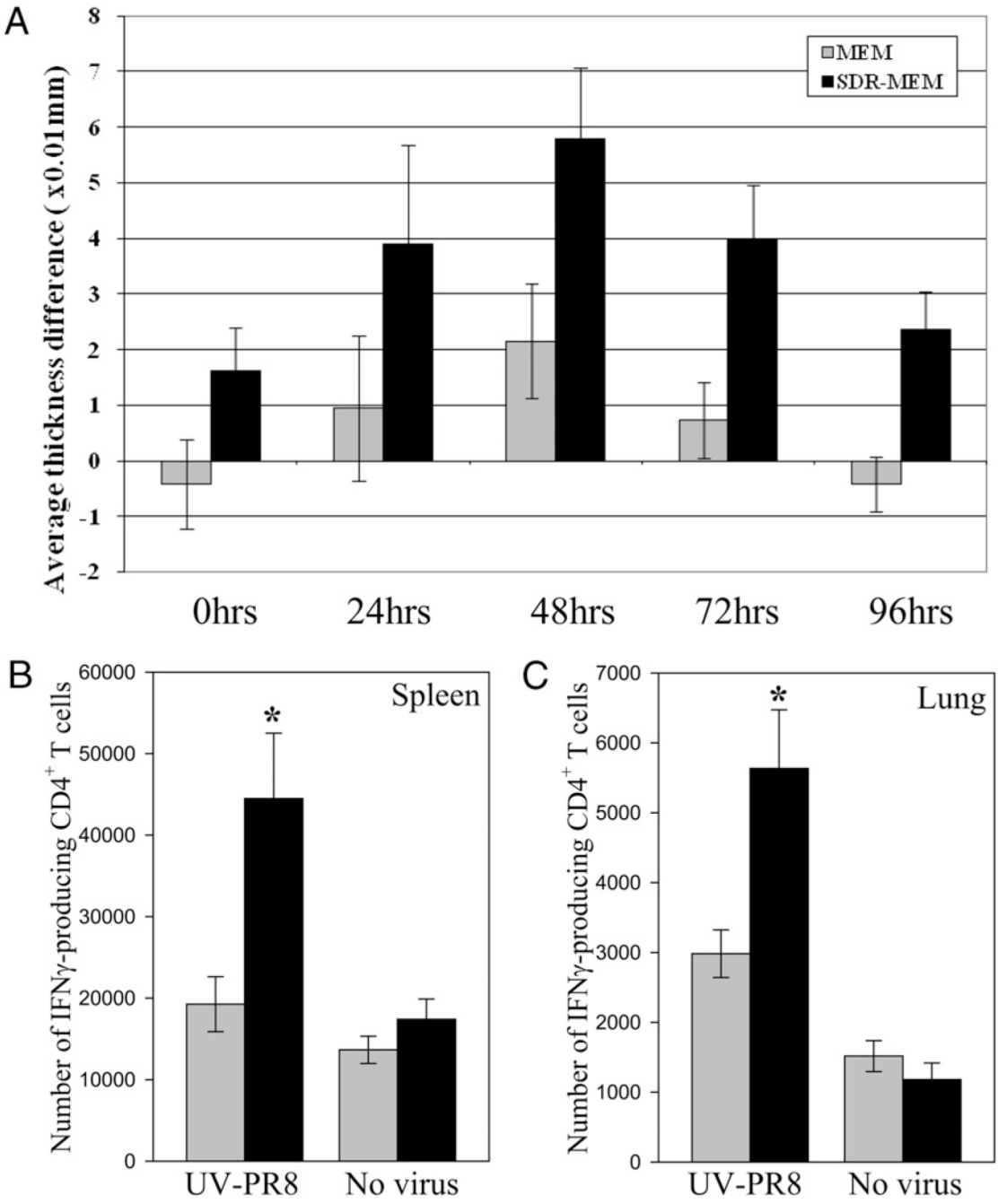

FIGURE 1.

In vivo and ex vivo screening assays confirmed enhanced anti-influenza immune responses in SDR-MEM mice. *A*, SDR-MEM mice developed a significantly greater DTH response over time versus nonstressed memory controls (MEM) following s.c. footpad injection with influenza A/PR/8/34 Ag. Each animal served as its own control, with one saline-injected and one Ag-injected footpad measured at 24-h intervals. Values were analyzed by subtracting the saline-injected footpad thickness from the Ag-injected footpad thickness at each time point (RM-ANOVA; SDR > MEM; $p < 0.001$; $n = 20$ per group). Values shown represent group mean ± SEM. This dataset is representative of four separate experiments. Mixed cell preparations from individual spleen (*B*) or lung (*C*) tissues taken from MEM or SDR-MEM

mice at 6 wk post-A/PR/8/34 infection were cocultured with UV-PR8 for 6 h and then the anti-influenza $CD4^+$ T cell response was assessed via flow cytometry. Organs were analyzed individually with $n = 5–7$ per group. $*p < 0.05$.

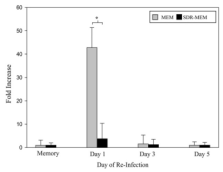

FIGURE 2.

Viral M1 gene expression was attenuated in SDR-MEM mice during reinfection. A/PR/8 virus gene expression was assessed by real-time PCR using primers and probes for the M1 gene of the influenza virus. The apical lobe of each lung was flash-frozen and processed for PCR analysis. Data are shown from four separate experiments, with $n = 9–21$ per group each day. Points represent group mean, and bars represent SEM for each point. $*p < 0.05$.

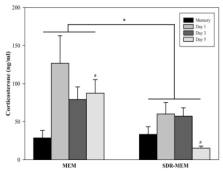

FIGURE 3.

HPA activation was reduced in SDR-MEM mice. Circulating corticosterone was measured throughout an influenza rechallenge. Mice were subjected to SDR, followed by primary influenza infection as described. Plasma was collected from trunk blood before rechallenge and at days 1, 3, and 5 postchallenge and was used to measure circulating corticosterone. Bars indicate the SEM of three to six mice per group. *MEM > SDR-MEM ($p < 0.05$ by ANOVA); $^{\#}$MEM, day 5 > SDRMEM, day 5 ($p < 0.05$).

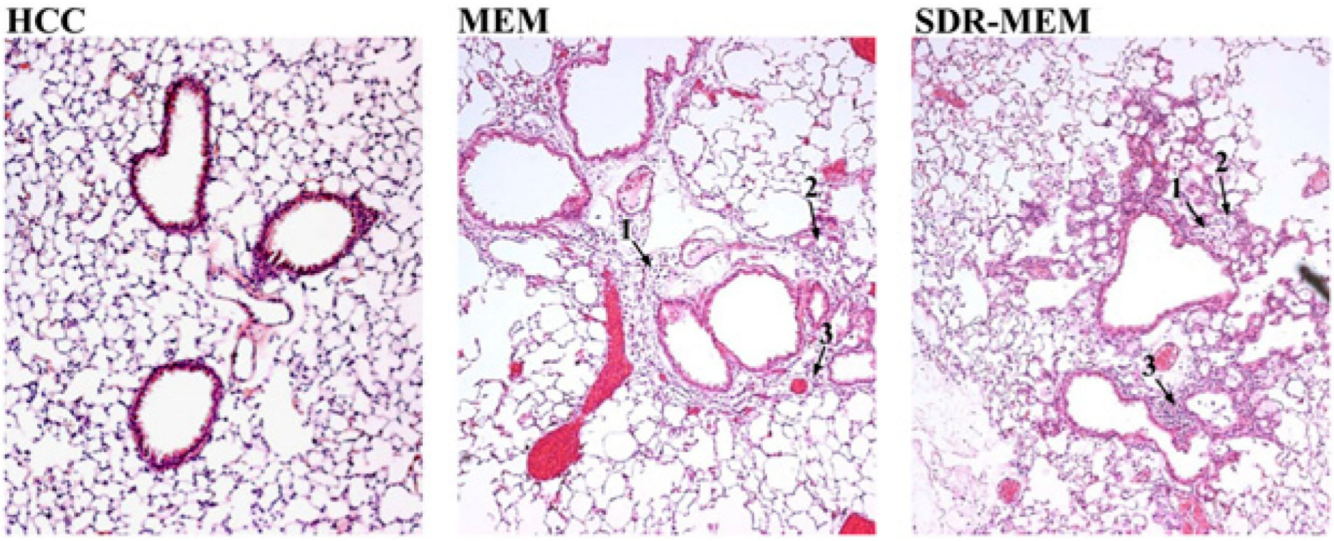

FIGURE 4.

Cellular infiltrate remained in lungs of MEM and SDRMEM mice at 6 wk after a primary influenza infection. Formalin-fixed paraffin-embedded lungs were prepared in 3 μm thick slices and stained with H&E. Sections shown are from the upper portion of the left lobe of the lung under a light microscope (original magnification ×10). Home cage control mice were age- and gender-matched naive controls. Tissue damage retained from the primary infection was evident in MEM and SDR-MEM lungs. 1, When compared with similar areas in MEM sections, more resident cells were consistently present in the pulmonary parenchyma of SDR-MEM mice; 2, SDR-MEM alveoli in these sections were often consolidated and filled with cellular and inflammatory debris consisting predominantly of mononuclear cells with fewer neutrophils; 3, some areas of perivascular cuffing remained in SDR-MEM lungs.

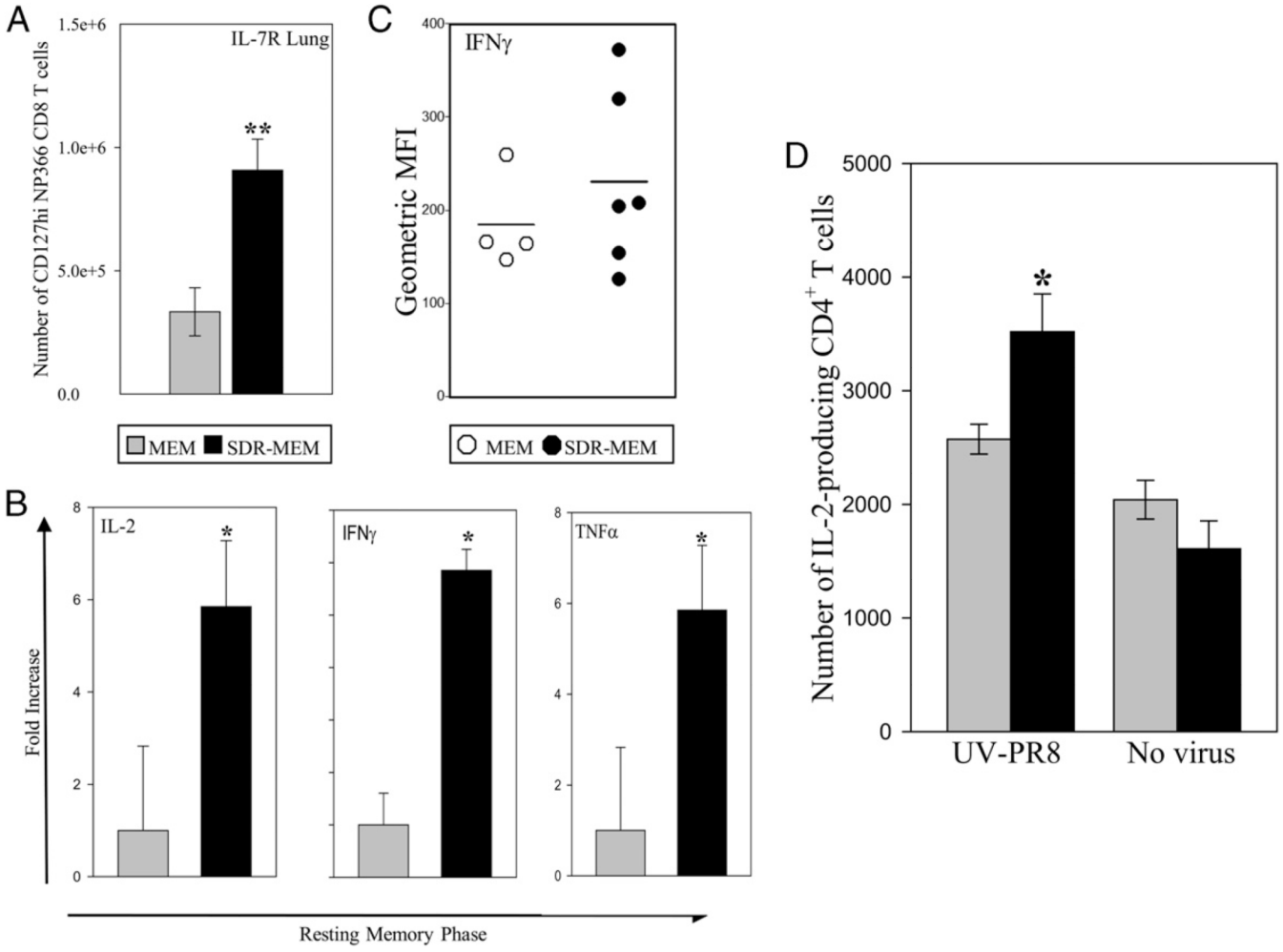

FIGURE 5.

SDR altered cellularity and function of lung parenchymal cells during resting memory. Mouse lungs were sampled 2–3 mo following resolution of a primary A/PR/8 infection. *A*, In SDR mice, a significant increase in the lung IL-$7R_{HI}$ $NP_{366}CD8^+$ memory phenotype population (**$p < 0.05$) was noted in the absence of active infection. *B*, Real-time PCR indicated increases in IL-2, IFN-γ, and TNF-α mRNA expression in lungs at this time. *$p < 0.05$. *C*, When lung $CD8^+$ T cells were stimulated ex vivo with NP366–74 peptide and stained for intracellular IFN-γ production, there was a suggestive, but nonsignificant, increase in the intensity of IFN-γ –producing $NP_{366–74}$ cells isolated from SDR-MEM lungs when mean fluorescence intensity (MFI) values were compared. Line indicates the mean MFI value for each group. *D*, In an effort to pinpoint the enhanced IL-2–producing lung cell population in SDR-MEM mice seen in *B*, whole lung preparations were cocultured with UV-PR8 for 6 h and then stained for surface markers and intracellular IL-2. In SDR-MEM mice, there was a significant increase (*$p < 0.05$) in the number of IL-2–producing $CD4^+$ T cells in lung tissue compared with MEM cell preparations.

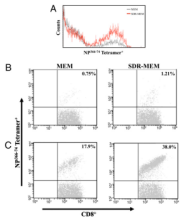

FIGURE 6.

SDR increased the proportion of $NP_{366–74}$ $CD8^+$ T cells of total $CD8^+$ T cells but did not alter the surface expression of the $NP_{366–74}$TCR. *A*, Staining intensity of the NP366 tetramer on memory $CD8^+$ T cells was not changed by exposure to SDR. The proportion of $NP_{366–74}CD8^+$ T cells detected during resting memory (*B*) and at the peak of the T cell response at day 5 of influenza reinfection (*C*) was affected by prior SDR experience. Populations shown were sequentially gated on lymphocytes, then $CD3^+CD8^+$ T cells, and finally on the $NP_{366–74}{}^+$ population. Percentages in the upper right quadrant represent the proportion of $NP_{366–74}CD8^+$ T cells to the total $CD8^+$ T cell population.

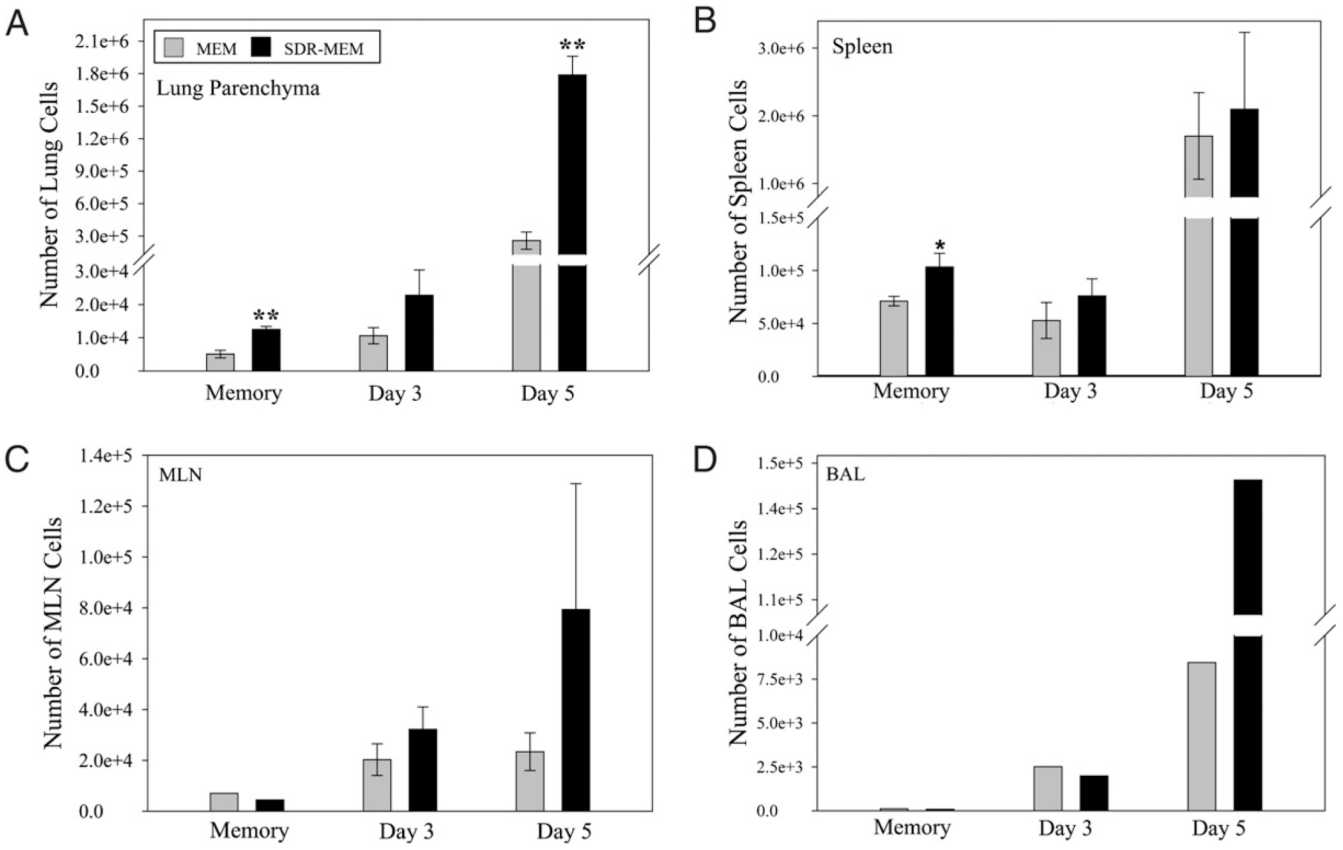

FIGURE 7.

SDR enhanced the size of the $NP_{366–74}$ $CD8^+$ memory T cell population. Mice were subjected to SDR and primary influenza infection as described. Flow cytometry data for a resting memory time point and days 3 and 5 after reinfection with A/PR/8 virus are shown. In *A–C*, bars represent the group mean ± SEM; $n = 4–6$ per group. In *D*, bars represent the measured value for the pooled sample by group each day. ANOVA indicated group-wise differences in the lung parenchyma (*A*) by stress, day postinfection, and stress*day (all $p < 0.001$). No overall differences were detected by ANOVA in the spleen samples; however, because the day 0 time point represents the resting memory population in the spleen, an individual *t* test was used to probe the data on that day. *SDR > MEM, $p < 0.05$ by individual *t* test; **SDR > MEM, $p < 0.01$ by individual *t* test.

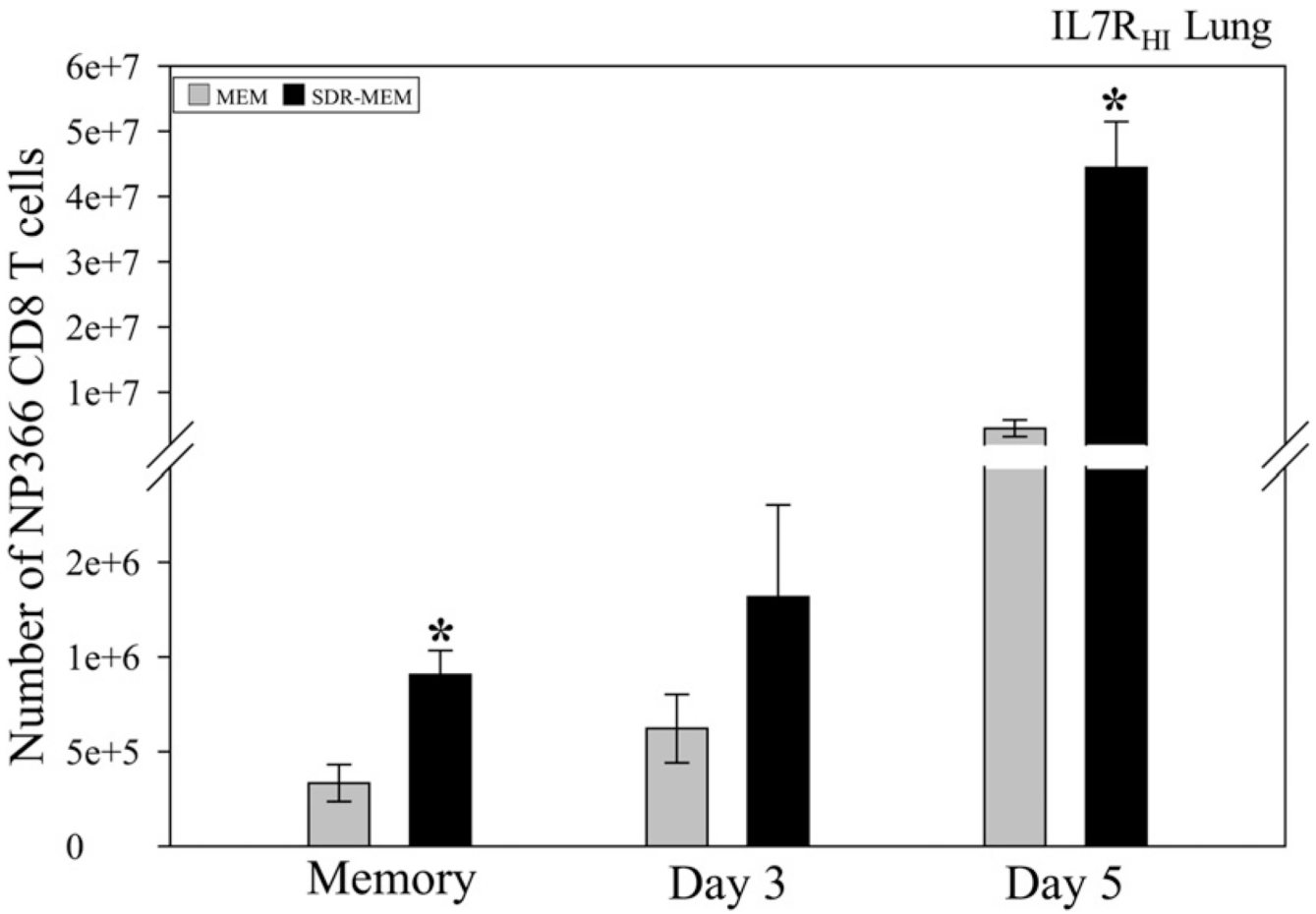

FIGURE 8.

Lung IL7R$_{HI}$NP$_{366–74}$CD8^{+} T cell population was augmented after SDR exposure. Lungs were processed for flow cytometry on the indicated days. Significant increases in the CD127$_{HI}$NP$_{366–74}$CD8^{+} T cell population were measured in the lung parenchymal tissue of SDR-MEM mice lung tissue during the memory phase and during rechallenge (stress, day, and stress*day effects; all $p < 0.0001$). Bars represent group mean ± SEM; $n = 4–6$ mice per group. *$p < 0.005$ by individual t test.

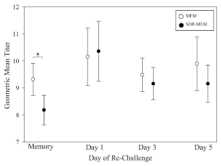

FIGURE 9.

Circulating serum IgG Ab GMTs were attenuated in SDRMEM mice only during resting memory. Retro-orbital blood samples were taken at 6+ weeks postprimary A/PR/8/34 infection and during homologous rechallenge. Circulating serum anti-influenza IgG Ab was assessed by ELISA (n = 10–20 per group). During resting memory, SDR-MEM mice had a >4-fold decrease in raw titer, and the 95% CI for the GMT was discordant from that of the SDR-MEM group, as confirmed by a two-sample t test (*p = 0.007). However, during A/PR/8/34 rechallenge, no intergroup differences in Ab titer were identified.

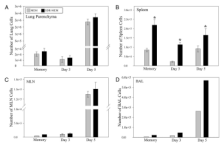

FIGURE 10.

SDR enhanced the size of the splenic $NP_{366–74}$ $CD8^+$ memory T cell population after influenza HKx31 priming. Mice were subjected to SDR and then infected intranasally with influenza X-31 virus. Six weeks after the primary infection, mice were challenged with the A/PR/8/34 virus. Flow cytometry data for a resting memory time point and days 3 and 5 after reinfection with A/PR/8/34 virus are shown. In *A–C*, bars represent group mean ± SEM; $n = 5–7$ per group. In *D* and the memory time point in *C*, the bars represent the measured value for the pooled sample by group each day, adjusted for the number of mice per group. ANOVA indicated group-wise differences in the spleen (SDR-MEM > MEM, $p < 0.001$), including significant increases in the SDR-MEM population at each individual time point ($*p < 0.05$). No differences were detected in the lung samples.